Physiological Research Pre-Press Article

^{99m}Tc-Sestamibi Uptake in Rat Skeletal Muscle and Heart: A Potential Physiological Explanation

G. ARSOS[1], A. KYPAROS[2,3], E. MORALIDIS[1], D. KYPAROS[2], S. GEORGA[1], S. SOTIRIADOU[2], C. MATZIARI[2], C. KARAKATSANIS[1]

[1]Department of Nuclear Medicine, Hippokration Hospital, Faculty of Medicine, Aristotle University of Thessaloniki, Greece
[2]Laboratory of Physiology, Department of Physical Education and Sports Science, Aristotle University of Thessaloniki, Greece
[3]Department of Biochemistry and Biotechnology, University of Thessaly, Greece.

Address for correspondence:

G. Arsos, MD
19 Zaka Str.
55236 Panorama
Thessaloniki, Greece
+30-2310-992808 (Phone)
+30-2310-992809 (Fax)
garsos@med.auth.gr (email)

Summary

The lipophilic cationic radiotracer ^{99m}Tc-sestamibi, known to be concentrated within mitochondria, is widely used for myocardial perfusion and to a lesser extent for muscle metabolism imaging. However, the exact distribution pattern in skeletal muscle has not been yet studied in detail. The present study aims at investigating the ^{99m}Tc-sestamibi uptake in rat skeletal muscle and myocardium in relation to their metabolic characteristics. ^{99m}Tc-sestamibi was i.v. administered in twenty adult male Wistar rats and uptake, as percent of injected dose per tissue gram (%ID/g), in the myocardium, soleus, extensor digitorum longus and gastrocnemius muscles was assessed 2 hours post injection. Muscle uptake was also correlated with myocardial uptake, muscle weight and body weight. Skeletal muscle ^{99m}Tc-sestamibi uptake was a small (9-16%) fraction of that found in myocardium (1.71±0.63 %ID/g). Among the three hindlimb muscles considered, the slow-oxidative soleus muscle showed the highest uptake (0.28±0.16 %ID/g). Metabolically diverse parts of the gastrocnemius muscle showed different uptake. Skeletal muscle uptake was positively correlated with myocardial uptake and both were negatively correlated with tissue and body weight. Evidence of matching exists between myocardial and muscle uptake, and both are size-dependent.

Key words: skeletal muscle, myocardium, ^{99m}Tc-sestamibi uptake, mitochondria

Introduction

Mitochondrial oxidative capacity plays a key role in muscle metabolism and performance. Muscle fibers are categorized according to their actomyosine adenosino-triphosphatase and mitochondrial oxidative enzymes activity (Saltin and Gollnick 1983). The histochemical profile of muscle fibers determines their performance characteristics. Accordingly, the major muscle functional properties, such as speed of contraction and fatigability, reflect their fiber-type composition. Activity pattern changes, or disease states, may alter mitochondrial metabolism and fiber-type distribution in muscles (Kwong and Vrbova 1981, Pette and Vrbova 1999).

Histochemical assessment of human muscle metabolism for both clinical and sports science purposes is well established. However, muscle biopsy, an invasive technique, is required and sampling errors may hamper representativeness (Lexell *et al.* 1985). Thus, noninvasive metabolic assessment of large muscle groups appears as attractive alternative.

Muscle imaging for medical or sports science use is gaining increasing interest; magnetic resonance imaging and spectroscopy have already been used for this purpose (Bangsbo *et al.* 1993, de Viser and Reimers 1994). Recently, muscle glucose metabolism has been explored by means of positron emission tomography (PET) using the glucose analogue [^{18}F]-2-fluoro-2-deoxy-d-glucose as a tracer (Nuutila and Kalliokoski 2000).

Methoxy isobutyl isonitrile is a lipophilic, cationic molecule delivered to tissues in proportion to regional blood flow and, due to transmembrane potentials, intracellularly retained within mitochondria (Piwnica-Worms *et al.* 1990). This compound labeled with technetium-99m (^{99m}Tc-hexakis 2-methoxy isobutyl isonitrile, ^{99m}Tc-sestamibi), is widely

applied in nuclear medicine for myocardial perfusion assessment, parathyroid gland localization and tumor imaging (Coakely *et al.* 1989, Maddahi *et al.* 1990, Actolun *et al.* 1992). Although myocardial uptake of ^{99m}Tc-sestamibi has been studied extensively, animal studies on the distribution of this radiotracer in skeletal muscles are lacking and only sporadic clinical publications on muscle metabolic imaging exist (Bostrom *et al.* 1993, Crane *et al.* 1993, Cittanti *et al.* 1997, Chang *et al.* 2005). The rat hindlimb muscles have been studied in detail with regard to their structural, histochemical, metabolic and functional aspects.

The purpose of the present study was to investigate the distribution of ^{99m}Tc-sestamibi among metabolically diverse rat hindlimb muscles and myocardium. In particular, we examined ^{99m}Tc-sestamibi uptake in the slow-twitch soleus, fast-twitch extensor digitorum longus and the mixed gastrocnemius muscles.

Methods

Animals

Twenty adult male Wistar rats with body weight ranging from 224 to 450 g (mean ± SD, 354 ± 52 g) were enrolled in this study. Rats were individually housed in standard Plexiglas cages on a 12-hour light/dark cycle in a room with controlled temperature (18-21 ^{o}C) and humidity (50-70%) and they had access to commercial rat chow and tap water *ad libitum.* The project was approved by the institutional review board. All procedures were in accordance with the European Union guidelines for the care and use of laboratory animals, as well as the "Principles of laboratory animal care" (NIH publication No. 86-23, revised 1985).

Radiopharmaceutical and standard preparation

A commercially available kit of lyophilized tetrakis (2-methoxy isobutyl isonitrile) (Cardiolite®), containing 1 mg of Cardiolite per vial, was labeled according to manufacturer's instructions by adding 1850 MBq (50 mCi) of freshly eluted ^{99m}Tc (as pertechnetate) to a final volume of 2.5 ml with saline. Radiochemical purity was over 95%. Individual doses were prepared in single-use insulin syringes. Syringes were weighed both before and after administration with four-digit accuracy. An extra syringe with similar activity to that of the administered dose was used for the preparation of a standard solution by diluting the content of the syringe in 500 ml of distilled water. Two samples of 1 ml each of the standard solution were drawn by precise pipeting.

Radiopharmaceutical administration

Under anesthesia with chloral hydrate (4.5% w/v, 450 mg·kg^{-1} body weight) injected intraperitoneally, the skin of the neck region was shaved and a small incision was

made on the right lateral side of the neck, disclosing the internal jugular vein. The radiopharmaceutical was administered through the vein by using insulin syringes with a 29G x ½-inch permanently attached needle (BD, USA), with the neck in overextended position under a magnifying lamp. The dose administered was 5.6 MBq (150 μCi) ^{99m}Tc-sestamibi per kg body weight. The volume of the injected dose was adjusted to approximately 0.1 ml by diluting with normal saline. The administration was followed by 0.5 ml normal saline flush. All animals were studied using a single vial of tracer. The radiopharmaceutical was administered within 4 hours of preparation. Injection was performed at a slow rate to ensure that no distention of the jugular vein was produced. After administration, gentle pressure was applied on the vessel for one minute by means of a wet piece of cotton, which was saved for later activity measurement.

Tissue harvesting

Based on ^{99m}Tc-sestamibi tissue kinetics data (Onoguchi *et al.* 2003), and the relatively short ^{99m}Tc half life (6.02 h), a 2-hour interval between radiopharmaceutical injection and tissue harvesting was considered as a reasonable compromise. During this period animals lay unconscious in supine position on the operating table. To maintain body temperature, rats were placed in the proximity of a diffuse heat source and covered with a "blanket" made of aluminum foil. Anesthesia was maintained by administering approximately 10% of the initial dose when necessary. The depth of anesthesia was assured by simple sensory tests, such as foot withdrawal when pinched and eye blinking when eyelid was touched. Two hours after tracer injection the animals were terminated by exsanguination through transthoracic cardiac puncture, and the soleus, extensor digitorum longus (EDL) and gastrocnemius (GA) muscles were removed bilaterally. The "red" part of

the GA (GA_{red}) was separated from the rest, "mixed" plus "white" part of the muscle ($GA_{mixed + white}$), according to Armstrong and Phelps (1984). The heart was also removed. Tissue harvesting was completed within 10-15 min.

Tissues were dissected free of connective tissue, rinsed with normal saline, blotted on absorbent paper, and weighed with four-digit accuracy. To check for potential extravasation of the radiopharmaceutical during injection, tissue blocks of approximately equal size including part of the jugular vein and surrounding tissues were bilaterally removed, weighed, and measured for radioactivity.

Measurements of activity and calculation of uptake

Radioactivity of the removed tissues and standards was measured in a well-type γ-counter (Oxford Instruments, USA) for 10 min. For the accurate assessment of tracer uptake, extravasation occurred during administration was considered and correction for physical decay of the ^{99m}Tc (half life time 6.02 hours) was performed. A detailed description of the uptake assessment has been provided elsewhere (Kyparos *et al.* 2006). Briefly, the uptake of radiopharmaceutical was calculated as a percentage of the injected dose (ID) per tissue gram as follows: Uptake (%ID/g) = k x C x Ws (mg) / Cs x WID (mg) x W (mg), where C, counts of muscle or myocardium; Cs, counts of 1 ml of standard solution; Ws, weight of standard; WID, weight of injected dose; W, weight of muscle or myocardium; k, proportionality constant dependent on standard dilution and sampling volumes. Relative uptake was defined as the ratio of muscle to myocardium uptake.

Statistics

Data were analyzed using SPSS, version 14 (SPSS, Chicago, IL, USA). Descriptive statistics were expressed as mean ± SD. The distribution of all dependent variables was

examined by the Shapiro–Wilk test and was found not to differ significantly from normal. To evaluate any differences in ^{99m}Tc-Sestamibi uptake among tissues, one-way ANOVA with repeated measures was carried out. When significant differences were found, *post hoc* pairwise comparisons were performed through simple main effect analysis. Linear regression analysis was used to assess the association between variables. To evaluate any difference in ^{99m}Tc-Sestamibi uptake between the GA_{red} and $GA_{mixed + white}$ portions of gastrocnemius muscle, paired student's *t*-test was applied. Paired student's *t*-test was also used to calculate any differences in ^{99m}Tc-Sestamibi uptake in the soleus, GA and EDL muscles between right and left hindlimb. Statistical significance was assigned at $P < 0.05$.

Results

No significant difference in weight or ^{99m}Tc-sestamibi uptake between left and right hindlimb muscles was detected ($P > 0.05$ in all muscles). Thus, only data from the muscles of the left hindlimb were analyzed. Both myocardium and hindlimb muscles weight displayed a strong linear correlation with body weight (Table 1).

Myocardial and muscle ^{99m}Tc-sestamibi uptake, as well as relative muscle/myocardial uptake, as percentage, are summarized in Table 2. Myocardial uptake was significantly higher than that of any hindlimb muscle ($P < 0.001$). Soleus muscle uptake was significantly higher than that in GA muscle ($P < 0.001$). Furthermore, GA_{red} showed significantly higher uptake than the rest ($GA_{mixed + white}$) of the muscle ($P < 0.001$). Soleus muscle uptake did not significantly differ from that of EDL muscle ($P = 0.18$).

Myocardium and muscle ^{99m}Tc-sestamibi uptake was negatively correlated with their own weight; this correlation was statistically significant for myocardium ($P < 0.01$) and GA ($P < 0.05$) muscle (Table 3). Myocardial and muscle uptake was also negatively correlated with rat body weight; statistical significance ($P < 0.05$) was noticed in myocardium, soleus and GA muscles. (Table 3, Fig 1).

^{99m}Tc-Sestamibi uptake in the hindlimb muscles examined, showed a fair positive correlation with myocardial uptake (r = 0.66, 0.59 and 0.64 for soleus, EDL and GA respectively, $P < 0.01$ in all cases) (Fig 2).

Discussion

The main finding of the present study is an escalation of ^{99m}Tc-sestamibi uptake in the examined tissues. Indeed, myocardial uptake was 6 times higher than that of the soleus muscle (1.71±0.63 vs 0.28±0.16 %ID/g). Soleus uptake was the highest among the three hindlimb muscles examined. This was two-fold higher than that of the GA $_{\text{mixed + white}}$ which showed the lowest ^{99m}Tc-sestamibi retention (0.14±0.07 %ID/g). EDL and GA $_{\text{red}}$ muscles had intermediate uptake values.

It is well established that ^{99m}Tc-sestamibi is specifically retained in mitochondria. Using homogenization techniques, 80-90% of ^{99m}Tc-sestamibi has been found within the mitochondrial fraction of myocardial and skeletal muscle cells (Crane *et al.* 1993). Moreover, using quantitative electron-probe x-ray microanalysis, a high mitochondrial concentration of the tracer has been reported in chick embryo heart cells (Backus *et al.* 1993).

Myocardial uptake of ^{99m}Tc-sestamibi in our animals (1.71±0.63 %ID/g) is comparable to the value of 1.15±0.47 %ID/g reported by Onoguchi *et al.* in rats, in a similar experimental setting (Onoguchi *et al.* 2003). The higher uptake value in our study may be the result of meticulous calculation of uptake by compensating for potential extravasation during administration (Kyparos *et al.* 2006). The high myocardial uptake is compatible with the high mitochondrial content reported in rat myocardium occupying approximately 36% of the myofiber volume (Page and McCallister 1973).

^{99m}Tc-sestamibi uptake values of EDL, a typical fast-twitch muscle, was found to be only slightly lower that of the soleus, a slow-twitch, fatigue-resistant muscle (0.23 ± 0.13 vs. 0.28 ± 0.16 %ID/g). This somehow surprising finding could be potentially related to the

very similar mitochondrial volume fractions reported in soleus and EDL rat muscles (8.4% vs. 7.5%, respectively) (van Ekeran *et al.* 1992). A lower mitochondrial volume fraction of 2.2% has been reported for the fast glycolytic (FG) muscle fibers of the rat GA muscle (Stonnington and Engel 1973). FG fibers make up 91% and 78% of the weight of the white and mixed rat GA muscle portions, respectively (Armstrong and Phelps 1984). This is consistent with the lowest ^{99m}Tc-sestamibi uptake found in the GA $_{\text{mixed + white}}$ portion of the GA muscle (0.14 ± 0.07 %ID/g).

An important issue in tracer distribution studies is the potential effect of the regional blood flow pattern. Owing to the high lipophilicity and the resulting easy crossing of cellular membranes, ^{99m}Tc-sestamibi is delivered to tissues in proportion to their regional blood flow. However, as ^{99m}Tc-sestamibi is lacking a “chemical microsphere” behavior, late intracellular retain is dynamically depended on sustained transmembrane potentials. Redistribution of ^{99m}Tc-sestamibi with high initial uptake which is declining over time has been shown in tissues with rich perfusion, such as the thyroid gland in humans (Santos *et al.* 2005).

In our study ^{99m}Tc-sestamibi was administered in anesthetized rats in supine position, thus having their hindlimbs unloaded. Depending on muscle functional role, standing position may result in significant blood flow inequalities among muscles. Blood flow studies with radioactive microspheres in rats in standing position showed that blood flow in the postural soleus muscle was on average 4.3 – 4.5 times higher than that of the fast EDL muscle (McDonald *et al.* 1983, Delp *et al.* 1991). In contrast, under hindlimb unweighting conditions, blood flow was very similar in all rat soleus, EDL, GA_{red}, GA $_{\text{mixed + white}}$ muscles, namely 8, 8, 8, 7 and 7 $ml \cdot min^{-1} \cdot 100\ g^{-1}$, respectively (McDonald *et al.*

1983). The later supports our suggestion that the variation in ^{99m}Tc-sestamibi uptake found in different muscles in our study can hardly be attributed to differences in blood flow pattern. Concerning myocardium, sustained high myocardial concentration of a freely moving radiotracer against negligible blood pool levels (Onoguchi *et al.* 2003), could also be explained by strong mitochondrial retention rather than by blood flow pattern.

Apart from the clear inter-tissue differences, intra-tissue variation of ^{99m}Tc-sestamibi uptake was also significant (Table 2). Since uptake had been expressed in %ID/g, minimization of the impact of tissue weight variability on uptake was expected. However, a weak to moderate negative linear correlation between tracer uptake and tissue weight was noticed (Table 3, Fig. 1). Given the close linear relationship between myocardium or muscle weight and body weight (Table 1), it was not surprising that a negative correlation between myocardial or muscle ^{99m}Tc-sestamibi uptake and body weight was also observed (Table 3, Fig 1).

These uptake-size relationships do not have straightforward explanations. At the muscle fiber level, a strong negative ($r = -0.933$) correlation between fiber size (measured as cross sectional area) and succinate dehydrogenase activity (a known mitochondrial activity marker) has been reported in the left ventricle of the rat myocardium, soleus and EDL muscles, suggesting size-specificity of SDH-activity (Nakatani *et al.* 1999). Capillary density, has also been shown to have a strong negative ($r = -0.81$) correlation with heart weight in rats (Kayar *et al.* 1986). In addition, skeletal muscle mitochondrial membrane surface has been shown to bear a negative allometric relation with body weight in mammals, with a -0.23 scaling exponent (Else and Hulbert 1985). Despite the relatively narrow body weight range (245-450 g) of the animals used in our study, changing body

size could also be a minor contributing factor in the modulation of the size-uptake relationship.

As a last observation, the moderately positive (r = 0.59 to 0.66) correlation between muscle and myocardial uptake may indicate a coordinated metabolic control over myocardial and muscle metabolism at the mitochondrial level.

A number of limitations may moderate the validity of our observations. First, direct morphometric measurements of muscle and myocardial mitochondria could provide a more robust link between metabolism and ^{99m}Tc-sestamibi uptake. Secondly, blood flow measurements with labeled microspheres could accurately distinguish between blood flow effect on cellular entrance and metabolic mitochondrial retention of the radiotracer. Finally, P-glycoprotein, a cellular membrane efflux pump, is known to diminish ^{99m}Tc-sestamibi uptake in cells by pumping the tracer out (Chen *et al.* 1997). However, minimal *mdr1* (the P-glycoprotein encoding gene) mRNA levels have been reported in heart and skeletal muscles in humans (Fojo *et al.* 1987).

Conclusion

In this study the distribution of ^{99m}Tc-sestamibi in rat hindlimb muscles and myocardium was investigated. The myocardium showed the highest uptake, followed by the slow twitch soleus muscle. The predominantly fast-twitch glycolytic part of the GA muscle had the lowest retention. These data may suggest that ^{99m}Tc-sestamibi uptake is related to the tissue metabolic characteristics and affected by size-uptake relationships.

Acknowledgment

Authors are thankful to Dr. N. Kokolis, Prof. of Physiology, Faculty of Veterinary Medicine, Aristotle University of Thessaloniki, for the generous hospitality in his lab where part of this experiment was conducted.

References

ACTOLUN C, BAYHAN H, KIR M**.** Clinical experience with Tc-99m MIBI imaging in patients with malignant tumors. Preliminary results and comparison with Tl-201. *Clin Nucl Med* **17**: 171-176, 1992.

ARMSTRONG RB, PHELPS RO**.** Muscle fiber type composition of the rat hindlimb. *Am J Anat* **171**: 259-272, 1984.

BACKUS M, PIWNICKA-WORMS D, HACKETT D, KRONAUGE J, LIEBERMAN M, INGRAM P, LEFURGEY A. Microprobe analysis of Tc-MIBI ine heart cells: calculation of mitochondrial membrane potential. *Am J Physiol* **256**: C178-C187, 1993.

BANGSBO J, JOHANSEN L, QUISTORFF B, SALTIN B. NMR and analytic biochemical evaluation of CrP and nucleotides in the human calf during muscle contraction. *J Appl Physiol* **74**: 2034-2039, 1993.

BOSTROM PA, DIEMER H, LEIDE S, LILJA B, BERGQVIST D. 99Tcm-sestamibi uptake in the leg muscles and in the myocardium in patients with intermittent claudication. *Angiology* **44**: 971-976, 1993.

CHANG YY, LEE CH, LAN MY, WU HS, CHANG CC, LIU JS. A new noninvasive test to detect mitochondrial dysfunction of skeletal muscles in progressive supranuclear palsy. *Ann N Y Acad Sci* **1042**: 76-81, 2005.

CHEN CC, MEADOWS B, REGIS J, KALAFSKY G, FOJO T, CARRASQUILLO JA, BATES SE. Detection of in vivo P-glycoprotein inhibition by PSC-833 using Tc-99m sestamibi. *Clin Cancer Res* **4**: 545-552, 1997.

CITTANTI C , COLAMUSSI P, GIGANTI M, ORLANDI C, UCCELLI L, MANFRINI S, AZZENA G, PIFFANELLI A. Technetium-99m sestamibi leg scintigraphy for non-invasive assessment of propionyI-L-carnitine induced changes in skeletal muscle metabolism. *Eur J Nucl Med* **24**: 762-766, 1997.

COAKELY AJ, KETTLE AG, WELLS CP, O' DOHERTY MJ, COLLINS REC. ^{99m}Tc sestamibi - a new agent for parathyroid imaging. *Nucl Med Commun* **10**: 791-794, 1989.

CRANE P, LALIBERTE R, HEMINWAY S, THOOLEN M, ORLANDI CL. Effect of mitochondrial viability and metabolism on technetium-99-sestamibi myocardial retention. *Eur J Nucl Med* **20**: 20-25, 1993.

DE VISSER M, REIMERS CD. Muscle Imaging. In: *Myology, Basic and Clinical*. ENGEL AG, FRANZINI-ARMSTRONG C (eds), McGraw-Hill, New York. 1994, pp. 795-806.

DELP MD, MANNING RO, BRUCKNER JV, ARMSTRONG RB. Distribution of cardiac output during diurnal changes of activity in rats. *Am J Physiol* **261**: 1487-1493, 1991.

ELSE PL, HULBERT AJ. Mammals: an allometric study of metabolism at tissue and mitochondrial level. *Am J Physiol* **248**: R415-R421, 1985.

FOJO AT, UEDA K, SLAMON DJ, POPLACK DG, GOTTESMAN MM, PASTAN I. Expression of a multidrug-resistance gene in human tumors and tissues. *PNAS* **84**: 265-269, 1987.

KAYAR SR, CONLEY KE, CLAASSEN H, HOPPELER H. Capillarity and mitochondrial distribution in rat myocardium following exercise training. *J Exp Biol* **120**: 189-199, 1986.

KYPAROS D, ARSOS G, GEORGA S, PETRIDOU A, KYPAROS A, PAPAGEORGIOU E, MOUGIOS V, MATZIARI C, KARAKATSANIS C. Asessment of Brown Adipose Tissue Activity in Rats by ^{99m}Tc-Sestamibi Uptake. *Physiol Res* **55**: 653-659, 2006.

KWONG WH, VRBOVA G. Effects of low-frequency electrical stimulation on fast and slow muscles of the rat. *Pflugers Arch* **391**: 200-207, 1981.

LEXELL J, TAYLOR C, SJÖSTRÖM M. Analysis of sampling errors in biopsy techniques using data from whole muscle cross sections. *J Appl Physiol* **59**: 1228-1235, 1985.

MADDAHI J, KIAT H, VAN TRAIN KF PRIGENT F, FRIEDMAN J, GARCIA EV, ALAZRAKI N, DEPUEY EG, NICHOLS K, BERMAN DS. Myocardial perfusion imaging with technetium-99m sestamibi SPECT in the evaluation of coronary artery disease. *Am J Cardiol* **66**: 55E-62E, 1990.

MCDONALD KS, DELP MD, FITTS RH. Effect of hindlimb unweighting on tissue blood flow in the rat. *J Appl Physiol* **54**: 1242-1248, 1983.

NAKATANI T, NAKASHIMA T, KITA T, HIROFUJI C, ITOH K, ITOH M, ISHIHARA A. Succinate dehydrogenase activities of fibers in the rat extensor digitorum longus, soleus, and cardiac muscles. *Arch Histol Cytol* **62**: 393-399, 1999.

NUUTILA P, KALLIOKOSKI K. Use of positron emission tomography in the assessment of skeletal muscle and tendon metabolism and perfusion. *Scand J Med Sci Sports* **10**: 346-350, 2000.

ONOGUCHI M, TAKAYAMA T, MIYATI T, TONAMI T, SMI Y, MAEHARA T. Comparison of 99mTc-MIBI uptakes on planar images with those in excised rats organs. *Nucl Med Commun* **24**: 47-54, 2003.

PAGE E, MCCALLISTER LP. Quantitative Electron Microscopic Description of Heart Muscle Cells. Application to Normal, Hypertrophied and Thyroxin-Stimulated Hearts. *Am J Cardiol* **31**: 172-181, 1973.

PETTE D, VRBOVA G. What does chronic electrical stimulation teach us about muscle plasticity? *Muscle Nerve* **22**: 666-677, 1999.

PIWNICA-WORMS D, KRONAUGE JF, CHIU ML. Uptake and retention of hexakis (2-methoxyisobutyl isonitrile) technetium(I) in cultured chick myocardial cells. Mitochondrial and plasma membrane potential dependence. *Circulation* **82**: 1826-1838, 1990.

SALTIN B, GOLLNICK PD. Skeletal muscle adaptability: significance for metabolism and performance. In: *Handbook of Physiology.* sect 10: *Skeletal Muscle.* PEACHY LD, ADRIAN RH GEIGER SR (eds), Bethesda, Maryland, 1983, pp. 555-631.

SANTOS AO, ZANTUT-WITTMANN DE, NOGUEIRA RO, ETCHEBEHERE ECSC, LIMA MCL, TAMBASCIA MA, CAMARGO EE, RAMOS CD. 199mTc-sestamibi thyroid uptake in euthyroid individuals and in patients with autoimmune thyroid disease. *Eur J Nucl Med Mol Imaging* **32**: 702-707, 2005.

STONNINGTON HH, ENGEL AG**.** Normal and denervated muscle. Amorphometric study of fine structure. *Neurology* **23**: 714-724, 1973.

VAN EKEREN GJ, SENGERS RCA, STADHOUDERS AM. Changes in volume densities and distribution of mitochondria in rat skeletal muscle after chronic hypoxia. *Int J Exp Path* **73**: 51-60, 1992.

FIGURE LEGENDS

Figure 1. Correlation of myocardial (left panel) and soleus (right panel) ^{99m}Tc-sestamibi uptake with body weight. r = –0.48, *P* = 0.033 for myocardium; r = –0.52, *P* = 0.019 for soleus muscle.

Figure 2. Correlation of soleus (left panel) and EDL (right panel) ^{99m}Tc-sestamibi uptake with myocardial uptake. r = 0.66, *P* = 0.0014 for soleus; r = 0.59, *P* = 0.0062 for EDL muscle.

Table 1. Body and tissues weight and correlation of tissues weight with body weight.

Tissue	**Weight (g)**		**r**	***P***
Total Body	354 ± 52	(224 – 450)		
Myocardium	1.017 ± 0.109	(0.712 – 1.150)	0.86	<0.001
Soleus	0.125 ± 0.027	(0.068 – 0.176)	0.93	<0.001
EDL	0.172 ± 0.031	(0.105 – 0.235)	0.98	<0.001
GA	1.977 ± 0.320	(1.273 – 2.494)	0.96	<0.001
GA_{red}	0.341 ± 0.072	(0.208 – 0.469)		
$GA_{mixed + white}$	1.632 ± 0.254	(1.064 - 2.026)		

Weight values represent mean ± SD; range in parentheses. EDL, extensor digitorum longus; GA, gastrocnemius; r, Pearson's correlation coefficient; *P*, significance.

Table 2. Myocardial and muscle ^{99m}Tc-sestamibi uptake, as well as relative muscle-to-myocardium uptake.

Tissue	**Uptake (%ID/g)**		**Relative uptake (%)**	
Myocardium	1.71 ± 0.63	(0.85 - 3.37)		
Soleus	0.28 ± 0.16	(0.08 - 0.65)	16.22 ± 6.81	(4.97 – 26.73)
EDL	0.23 ± 0.13	(0.06 - 0.46)	13.62 ± 6.90	(4.30 – 29.02)
GA	0.15 ± 0.08	(0.05 - 0.28)	08.96 ± 3.68	(2.95 – 15.83)
GA $_{red}$	0.18 ± 0.10	(0.05 - 0.35)	10.71 ± 4.76	(3.46 – 18.91)
GA $_{mixed + white}$	0.14 ± 0.07	(0.05 - 0.27)	08.68 ± 3.50	(2.84 – 15.77)

Values represent mean ± SD; range in parentheses. EDL = extensor digitorum longus, GA = gastrocnemius.

Table 3. Correlation of myocardial and muscle ^{99m}Tc-sestamibi uptake with tissue weight and rat body weight.

	Uptake - tissue weight		**Uptake - body weight**	
Tissue	r	*P*	r	*P*
Myocardium	–0.63	0.003**	–0.48	0.033*
Soleus	–0.36	0.118	–0.52	0.019*
EDL	–0.33	0.162	–0.28	0.229
GA	–0.53	0.012*	–0.49	0.027*

Values represent mean ± SD. EDL, extensor digitorum longus; GA, gastrocnemius; r, Pearson's correlation coefficient; *P*, significance; *, < 0.05; **, < 0.01.

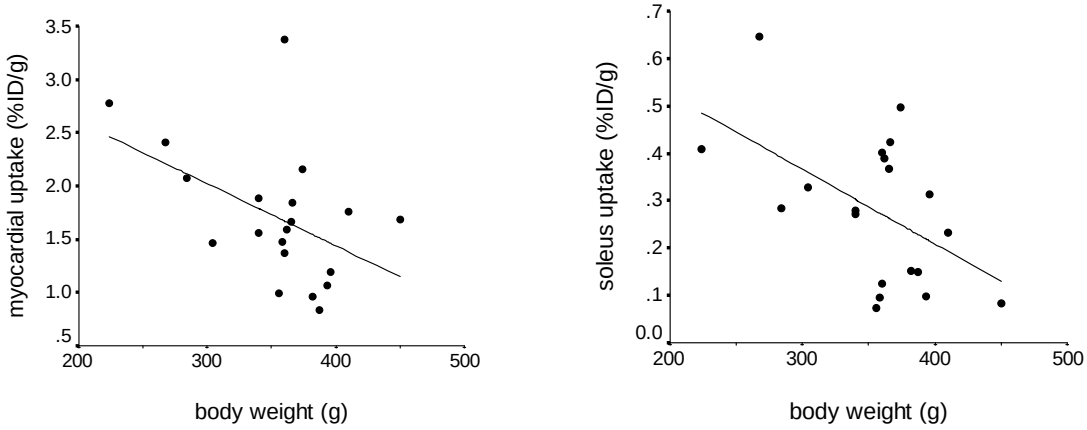
myocardial uptake (%ID/g)
3.5
3.0
2.5
2.0
1.5
1.0
.5
200
300
400
500
body weight (g)
soleus uptake (%ID/g)
.7
.6
.5
.4
.3
.2
.1
0.0
200
300
400
500
body weight (g)

Figure 1.

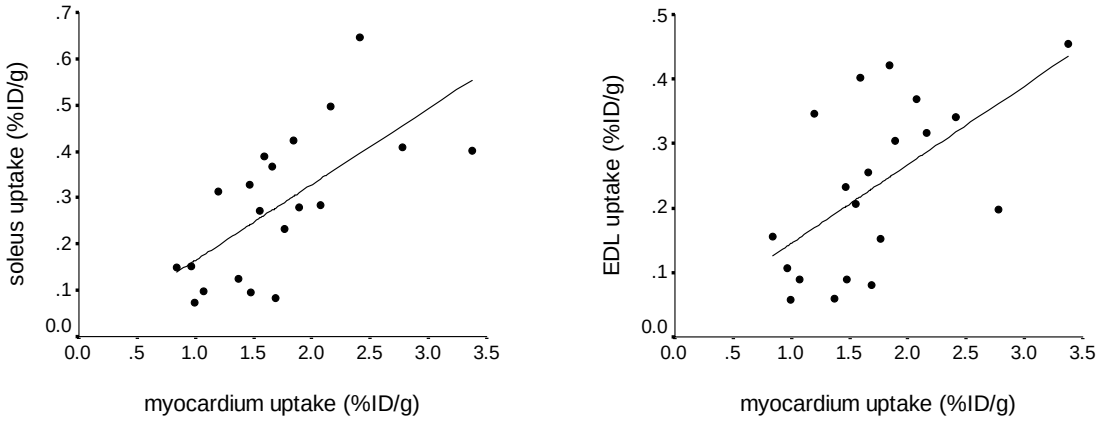
soleus uptake (%ID/g)
.7
.6
.5
.4
.3
.2
.1
0.0
0.0
.5
1.0
1.5
2.0
2.5
3.0
3.5
myocardium uptake (%ID/g)
EDL uptake (%ID/g)
.5
.4
.3
.2
.1
0.0
0.0
.5
1.0
1.5
2.0
2.5
3.0
3.5
myocardium uptake (%ID/g)

Figure 2.